

Current sheet structure near magnetic X-line observed by Cluster

A. Runov,¹ R. Nakamura,¹ W. Baumjohann,¹ R. A. Treumann,² T. L. Zhang,¹
M. Volwerk,¹ Z. Vörös,¹ A. Balogh,³ K.-H. Glaßmeier,⁴ B. Klecker,² H. Rème,⁵ and L. Kistler⁶

Received 6 December 2002; revised 31 March 2003; accepted 29 April 2003; published 10 June 2003.

[1] During the interval 0947–0951 UT on 1 October 2001, when Cluster was located at $X_{GSM} = -16.4 R_E$ near $Z_{GSM} = 0$ in the pre-midnight magnetotail, the Cluster barycenter crosses the neutral sheet four times. High speed proton flow, with reversal from tailward to Earthward, was detected during the crossings. Using a linear gradient/curl estimator technique we estimate current density and magnetic field curvature within the crossings. These observations exhibit the tailward passage of an X-line over the Cluster tetrahedron. These current sheet has a bifurcated structure in the regions of tailward and earthward flows and a flat and/or slightly bifurcated thin current sheet in between. A distinct quadrupolar Hall magnetic field component was observed. **INDEX TERMS:** 2740 Magnetospheric Physics: Magnetospheric configuration and dynamics; 2744 Magnetospheric Physics: Magnetotail; 2764 Magnetospheric Physics: Plasma sheet; 7835 Space Plasma Physics: Magnetic reconnection. **Citation:** Runov, A., et al., Current sheet structure near magnetic X-line observed by Cluster, *Geophys. Res. Lett.*, 30(11), 1579, doi:10.1029/2002GL016730, 2003.

1. Introduction

[2] Detection of a reconnection region and studying its current/plasma sheet structure is difficult using single spacecraft measurements. Cluster, being a four spacecraft constellation, offers a possibility to study the spatial structure of the plasma sheet near and/or within the reconnection region.

[3] The standard macroscopic picture of magnetic reconnection includes an X-type magnetic neutral line, cold plasma inflow toward the neutral line and high speed accelerated plasma outflow. The outflow region is bounded by branches of a bifurcated current sheet. This scheme is supported by MHD simulations [e.g., Ugai and Tsuda, 1977; Sato and Hayashi, 1979] and analytical solutions [e.g., Semenov et al., 1998].

[4] As it was proposed by Sonnerup [1979], ions and electrons move differently around the X-line, and this decoupling results in a Hall current system near the X-line. Terasawa [1983] found the Hall component of the magnetic field in a tearing mode stability analysis. It was also shown in Hall-MHD [e.g., Lottermoser and Scholer, 1997], hybrid [e.g., Lottermoser et al., 1998; Nakamura et al., 1998] and

PIC [Hesse et al., 2001; Pritchett, 2001] simulations that a magnetic reconnection produces a quadrupolar out-of-plane component of the magnetic field. The characteristic scale of this structure is of the order of the ion inertial length. Measurements on-board the Geotail [Nagai et al., 2001] at $X \sim 25-30 R_E$ and Wind [Øieroset et al., 2001] ($X \sim 60 R_E$) showed the quadrupolar Hall magnetic field near the magnetic reconnection region. But it was not possible to estimate the characteristic scale of the Hall region using single spacecraft measurements.

[5] The purpose of this paper is to present multi-point observations of the magnetic reconnection region, detected by Cluster on 1 October 2001. Four-point measurements allow analyzing the current sheet structure in the reconnection region and estimating the characteristic scales for different parts of this region.

2. Observations and Data Analysis

[6] At 0947–0951 UT on 1 October 2001, Cluster was located at $[-16.4; +8; 0.5] R_E$, GSM coordinates are used overall this paper. The Cluster tetrahedron configuration is shown in Figures 1a and 1b. During a half-hour long interval 0930–1000 UT Cluster repeatedly crosses the neutral sheet, located approximately in the $Z_{GSM} = 0$ plane. FGM [Balogh et al., 2001] 1-s resolution data for 0947–0951 UT are shown in Figures 1c–1e. It is seen from FGM data and from the relative Cluster positions that during 0947–0951 UT B_x from s/c 1 is larger than B_x from the more southern s/c. Except for a short-time perturbation at $\sim 0947:40-0947:45$ UT, the southernmost s/c 3 detects the smallest B_x . The magnetic field gradient is thus mainly directed along Z_{GSM} , and the GSM system is suitable for studying this event.

[7] Data from the CIS experiment [Rème et al., 2001] in the time interval 0947–0951 UT show a reversal of the proton bulk flow from tailward to earthward. Figures 1f, g show the X_{GSM} and Z_{GSM} components of the perpendicular velocity vector $\mathbf{V}_{\perp p} = \mathbf{b} \times (\mathbf{V}_p \times \mathbf{b})$, where $\mathbf{b} = \mathbf{B}/|B|$, and \mathbf{V}_p is proton bulk velocity from CIS/CODIF. Spin-averaged (~ 4 , s) resolution data are used. Maximum (minimum) proton bulk velocity value from s/c 1, 3, 4 are ~ 900 (-700) km s^{-1} for the Earthward and tailward flows, respectively, which is $\sim 0.5 V_A$, with V_A the Alfvén speed in the lobe ($B \sim 25$ nT, $N_p \sim 0.1 \text{ cm}^{-3}$, according to Cluster 1).

[8] During the interval 0947–0951 UT Cluster 2, 3, 4 cross the neutral sheet four times. Cluster 1 stays in the northern hemisphere (NH) in close vicinity of the neutral sheet. During the first crossing (denoted as “A”) Cluster 2, 3 and 4 traverse the neutral sheet from NH into the southern hemisphere (SH). They detect fast tailward proton bulk flows concentrated near $B_x \sim 0$. This tailward flow follows a large amplitude bipolar variation of B_z , which is the

¹Institut für Weltraumforschung der ÖAW, Graz, Austria.

²Max-Planck-Institut für extraterrestrische Physik, Garching, Germany.

³Imperial College, London, UK.

⁴TU Braunschweig, Braunschweig, Germany.

⁵CESR/CNRS, Toulouse, France.

⁶University of New Hampshire, Durham, NH, USA.

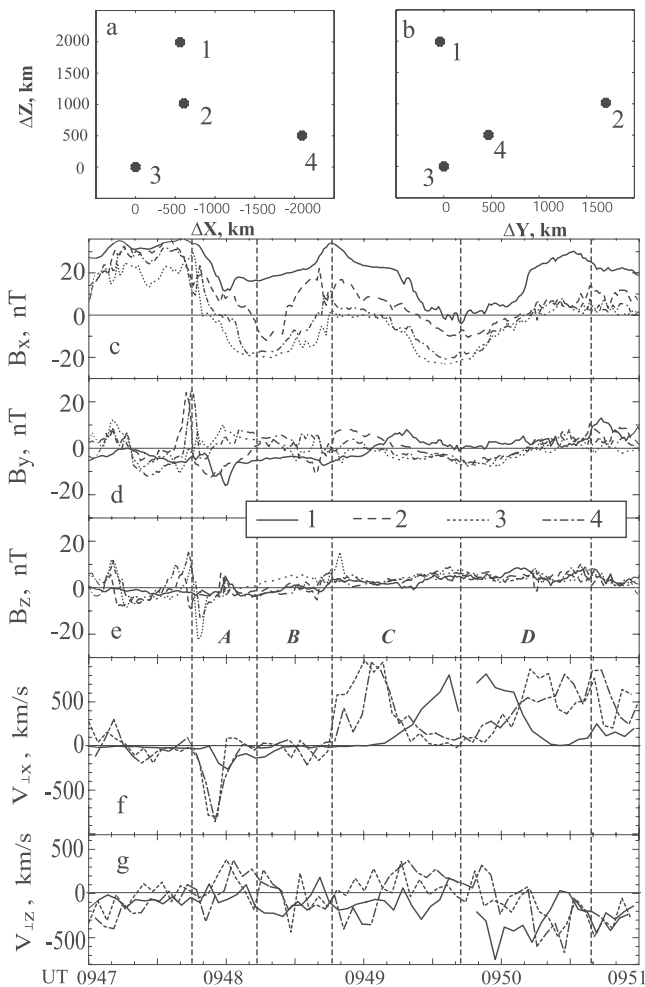


Figure 1. Cluster tetrahedron configuration (a,b) and measurements: GSM-components (c–e) of the magnetic field from Cluster/FGM, 1-s resolution, X_{GSM} (f) and Z_{GSM} (g) components of perpendicular proton bulk velocity vector from Cluster/CIS-CODIF, spin resolution, versus UT.

signature of a plasmoid. The value of B_z measured by s/c 2, 3 and 4 during the tailward flow interval *A* are mostly negative with minima of -9 , -22 , -13 nT, respectively.

[9] During the next crossing, marked “*B*”, s/c 2, 3 and 4 return from SH to NH. It is clearly seen from the B_x traces of the spacecraft that the current sheet becomes thinner during the traversal from *A* to *B*. During interval *B*, the X -component of \mathbf{V}_\perp is about zero. Cluster 1, staying in NH, detects a negative Z component $V_{\perp z}$, while s/c 4 in SH sees a positive $V_{\perp z}$ in between *A* and *B*. The B_z components at s/c 1, 2, and 4 are about zero. In contrast, $B_z \sim 5$ nT at s/c 3 with a peak value of 16 nT at 0948:50 UT.

[10] During interval *C* all four Cluster spacecraft cross the neutral sheet from NH to SH and detect fast Earthward proton bulk flows, focused at $B_x \sim 0$. The B_z -components are all positive with a tendency to grow. The maximum value of B_z is ~ 5 nT. The Z -component of the proton bulk velocity s/c 1 and 4 changes from negative to positive. The next SH \rightarrow NH crossing (*D*) is characterized by a large positive $V_{\perp x}$ and significant negative $V_{\perp z}$, and $B_z \sim 5$ – 8 nT.

[11] The correlation between the magnetic field measurements of the four spacecraft was high (correlation coeffi-

cient $0.82 < R < 0.95$). Hence all spacecraft stay in the same physical region, and the linear gradient and curl estimator technique [Chanteur, 1998] can be applied. Figure 2 shows the magnetic field components in the tetrahedron barycenter (upper panel), the $\mathbf{curl} \mathbf{B}$ components, X and Y GSM components of the magnetic field curvature vector $\mathbf{curv} \mathbf{B} = (\mathbf{b} \cdot \nabla)\mathbf{b}$, magnetic field divergence $div \mathbf{B}$, and X - and Z -components of the bulk proton flow from the mean value of the s/c 1, 3 and 4 CIS/CODIF measurements. The y -component of $\mathbf{curl} \mathbf{B}$ has a maximum value of ~ 16 – 20 nT/ 10^3 km ($j_y \sim 12$ – 15 nA m $^{-2}$) in the transition region between the tailward and earthward flow regions. There are significant peaks of in-plane (X and Z) components of the $\mathbf{curl} \mathbf{B}$ over crossings *A* and *B*, which may be interpreted as Hall-current branches: positive X - and negative Z -components in the NH \rightarrow SH crossing during tailward flow (*A*) and negative X , and weak positive Z components of the current density in the crossings *C* and *D* associated with strong earthward ion flow (see the schematic representation of the Hall current system by Nagai *et al.* [2001]). It should be noted that $div \mathbf{B}$, which is a measure of the accuracy of the calculation, ranges between ± 5 nT/ 10^3 km, except for a peak up to -10 nT/ 10^3 km at 0948:40 UT.

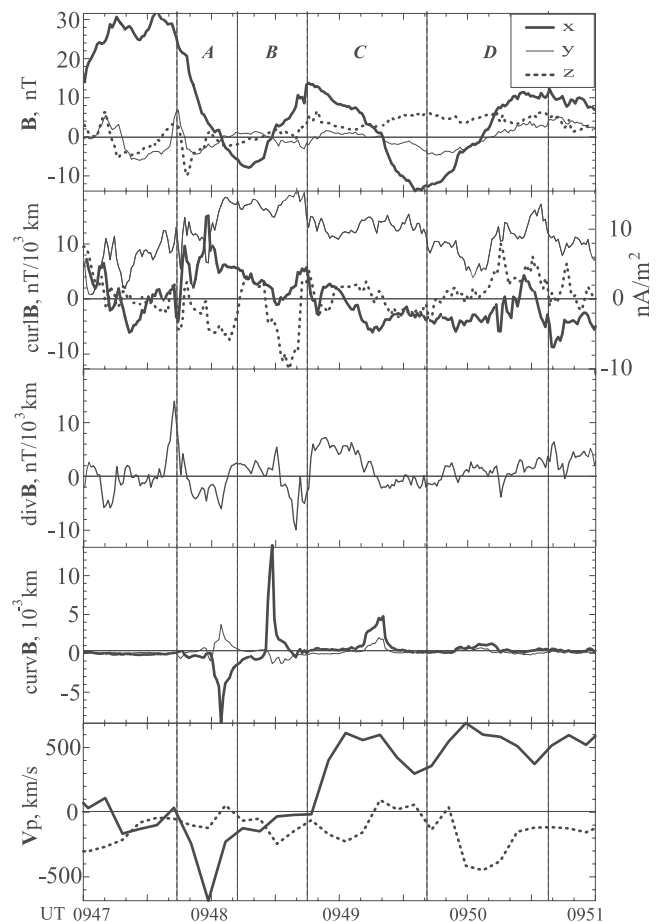


Figure 2. Cluster measurements at the tetrahedron barycenter. From top to bottom: components of the magnetic field, components of $\mathbf{curl} \mathbf{B}$ vector, the magnetic field divergence, X and Y components of the magnetic field curvature vector, and proton bulk velocity as a mean value of s/c 1, 3 and 4 measurements versus UT.

[12] The X -component of the magnetic field curvature dominates all four neutral sheet crossings. Moreover, the tailward flow (A) is associated with a large negative X -component in the magnetic field curvature, while during the crossings B , C and D the X -component of the curvature is positive. Thus, the magnetic field loop associated with tailward proton flow is open in the tailward direction, and the loop associated with earthward flow is open toward Earth. These observations can be interpreted as the tailward passage of an X-line region over Cluster. The nonzero Y component of the magnetic curvature vector probably results from the small tilt of the current sheet with respect to the $Z_{GSM} = 0$ plane. The Z -component of the curvature vector (not shown) is negligibly small.

[13] CIS/CODIF onboard s/c 1, 3 and 4 detected tailward moving protons of energy 1–10 keV (s/c 1) and ~ 10 keV (s/c 3 and 4) during crossing A , 0.1–1 keV for s/c 1, which stays at the level of $B_x \sim 20$ nT, and ~ 1 keV for s/c 3 and 4 during crossing B , and ≥ 10 keV during crossings C and D (not shown). These observations conform to ion flow in the vicinity of an X-line: cold (lobe) plasma inflow (B) and accelerated plasma outflow (A , C , D).

[14] Using the calculated $\mathbf{curl} \mathbf{B}$, we analyzed the current sheet structure near the X-line. Figure 3 shows the y -component of $\mathbf{curl} \mathbf{B}$, which results mostly from the magnetic field gradient along Z_{GSM} , versus B_x in the tetrahedron barycentre (B_{xc}). During crossing A , the Y -component of the current density associated with the tailward ion flow tends to decrease when $B_{xc} \rightarrow 0$. After jumping to a large value, which probably is a temporal effect, $j_y \sim (\mathbf{curl} \mathbf{B})_y$ has a local minimum near $B_{xc} \sim 0$ –5 nT in crossing B (Figure 3, thick curve, marked by bullets). It should be noted that the estimate of $\mathbf{curl} \mathbf{B}$ during the interval 0948:25–0948:35 UT, when s/c 2, 3, and 4 are in SH, and s/c 1 stays in NH, is of minimum accuracy. The linear estimate of the magnetic field divergence for this interval yields absolute values of 1–5 nT/10³km, an order of magnitude less than the estimate of $\mathbf{curl} \mathbf{B}_y$, but comparable with the difference between the maximum and minimum values of j_y in crossing B . Thus, the current density during this interval has a rather flat distribution with a tendency to decrease when $B_x \rightarrow 0$.

[15] The value of j_y drops to a smaller value between crossings B and C and exhibits a flat profile (curve marked

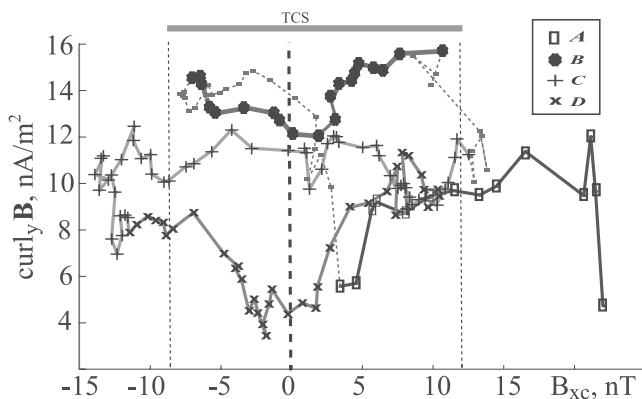


Figure 3. Current sheet structure in the vicinity of the X-line: the Y -component of $\mathbf{curl} \mathbf{B}$ (cross-tail current density) versus B_x in the tetrahedron barycentre.

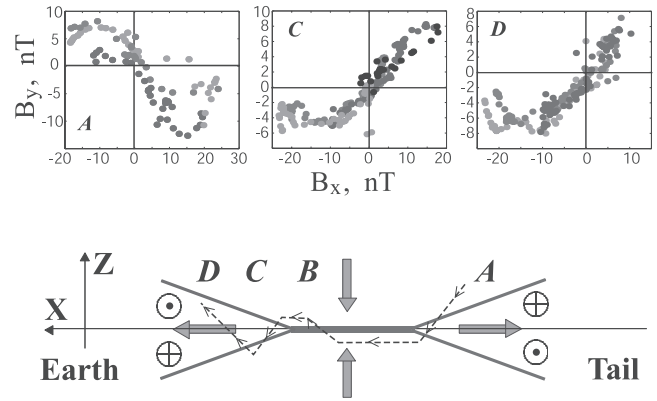


Figure 4. The out-of-plane Hall magnetic field component B_y versus B_x over neutral sheet crossings A , C and D (upper panel), and a sketch of reconnected current sheet structure with Hall currents. \odot and \oplus denote the B_y direction; dotted line shows schematic representation of the Cluster barycentre trajectory.

by “+” sign) during crossing C . This is associated with earthward proton flow. In crossing D (curve marked by “x”) the j_y profile has a pronounced minimum at $B_{xc} \sim 0$.

[16] Figure 4 shows scatter plots of the out-of-plane B_y component versus B_x for crossings A , C and D . During the NH \rightarrow SH crossing A , B_y changes from being positive at $B_x > 0$ (NH) to negative at $B_x < 0$ (SH). The crossings C (NH \rightarrow SH) and D (NH \rightarrow SH) are characterized by positive B_y at $B_x > 0$ and negative B_y at $B_x < 0$. These results are consistent with the presence of Hall currents. A sketch of the reconnected current sheet structure including the Hall magnetic field near the X-line is given in the bottom panel of Figure 4.

3. Discussion

[17] We interpret the Cluster observations of 1 October 2001 at 0947–0951 UT in terms of an X-line in tailward motion past the spacecraft. The Cluster four-point measurements allow us to calculate the magnetic field curvature and curl and to analyze the current sheet structure near the X-line. The actual value of the current density $\mathbf{j} = \mu_0^{-1} \mathbf{curl} \mathbf{B}$ may be underestimated because the inter-spacecraft separations are too large in order to detect any small-scale current structures.

[18] The current sheet profiles in the crossings A and D are consistent with a bifurcated current structure in both reconnection outflow regions, as predicted by MHD/Hall-MHD and kinetic simulations of the reconnection process, as well as some analytical solutions. A double-peak current structure had already been detected in the distant tail by *Hoshino et al.* [1996] from the statistical analysis of Geotail measurements. It was interpreted there in terms of a pair of Petschek-type shock waves formed in localized reconnection. *Asano* [2001] showed that the cross-tail current has a bifurcated structure in the post-plasmoid plasma sheet in agreement with simulation results of *Arzner and Scholer* [2001]. Recently, *Nakamura et al.* [2002], *Runov et al.* [2002], and *Sergeev et al.* [2002] observed bifurcated current sheets in the Cluster observations. In contrast to this paper, in those cases the bifurcation could not be directly attributed to magnetic reconnection.

[19] The thick curve, corresponding to crossing B in Figure 3 indicates that the current density in this crossing is higher than during the other crossings. This intense current is localized in the B_x interval $-10 \text{ nT} < B_x < 12 \text{ nT}$. From the gradient estimate one finds a rough value of $\lambda \sim 500\text{--}600 \text{ km}$ for the half-width of the current, in agreement with the estimate obtained from the fit to a Harris-type model [Nakamura *et al.*, 2002]. We may therefore conclude that the Cluster observations support that the reconnection region at 0947–0951 UT has the structure sketched in Figure 4 and exhibits two outflow regions that are bounded by bifurcated currents, and a comparably thin current sheet in the center. The TCS was observed by Cluster during the 30 s long interval 0948:07–0948:40 UT. Referring to the average value of $\langle V_x \rangle \approx -200 \text{ km s}^{-1}$ during this interval we get as an estimate of the length of the TCS along X a value of $\sim 6000\text{--}7000 \text{ km}$, about 10 ion Larmor radii (calculated for 10-keV ions in a 20 nT field). It should be noted that the structure of the TCS differs from a Harris sheet. The current density profile has a local minimum at $B_x \sim 0$.

[20] The Y -component of the magnetic field has a quadrupolar spatial distribution. This behavior of B_y near the magnetic X-line is predicted by Hall-MHD, hybrid and kinetic simulations of the reconnection process and is an indication for the magnetic X-line being detected [e.g., Nagai *et al.*, 2001]. The observations allow for an estimate of the ion inertial length d_i , using the calculated gradient of the magnetic field. One finds that $d_i \sim 1742, 1451, \text{ and } 2540 \text{ km}$ for crossings A, C and D , respectively.

4. Concluding Remarks

[21] Magnetic reconnection relies on microscopic aspects of magnetic field and particle dynamics. In the first place it is the dynamics of the electrons that determines the reconnection process [for a recent account see e.g., Sitnov *et al.*, 2002]. Decoupling of the electron motion from ions takes place on the ion inertial scale near the X-line. This decoupling gives rise to Hall currents and generates a Hall B_y field component. It thus can be detected in a comparably large volume, while the decoupling of the electrons from the magnetic field takes place on the electron inertial scale and thus usually escapes observation. One should, however, keep in mind that the Hall field is but an indication of decoupling of electron and ion dynamics. In the reconnection process itself it plays a little role as it merely rotates the total field. In this sense the characteristic ion and electron inertial lengths are the crucial parameters of the physical processes in the reconnection region. In our analysis of Cluster X-line observations on 1 October 2001, Cluster was able to resolve some of the fine structure of the reconnection region and to determine these scales. The accuracy of the estimates of characteristic lengths as well as the scales of the gradient and curl is still relatively low. It will be essentially higher with upcoming smaller inter-spacecraft separation. Nonetheless, for the event under consideration in this communication we were able to draw a consistent picture of the structure of the tail reconnection region in relation to currents, flows, and the geometry of the magnetic field.

[22] **Acknowledgments.** We thank H.-U. Eichelberger, G. Laky, and Y. Bogdanova for helping Cluster data analysis, and T. Terasawa, V. Sergeev, M. Sitnov, V. Semenov, T. Nagai, and M. Fujimoto for helpful discussion and comments. We acknowledge the CSDS and the World Data Center for Geomagnetism in Kyoto.

References

- Arzner, K., and M. Scholer, Kinetic structure of the post plasmoid plasma sheet during magnetic reconnection, *J. Geophys. Res.*, *106*, 3827, 2001.
- Asano, Y., Configuration of the thin current sheet in substorms, Ph.D. thesis, Univ. Tokyo, 2001.
- Balogh, A., et al., The Cluster magnetic field investigation: overview of in-flight performance and initial results, *Ann. Geophys.*, *19*, 1207, 2001.
- Chanteur, G., Spatial interpolation for four spacecraft: Theory, In *Analysis Methods for Multi-Spacecraft Data*, edited by G. Paschmann and P. Daly, ISSI Scientific Report SR-001, ISSI/ESA, 349–369, 1998.
- Hesse, M., J. Birn, and M. Kuznetsova, Collisionless magnetic reconnection: Electron processes and transport modeling, *J. Geophys. Res.*, *106*, 3721, 2001.
- Hoshino, M., A. Nishida, T. Mukai, Y. Saito, and T. Yamamoto, Structure of plasma sheet in magnetotail: Double-peaked electric current sheet, *J. Geophys. Res.*, *101*, 24,775, 1996.
- Lottermoser, R.-F., and M. Scholer, Undriven magnetic reconnection in magnetohydrodynamics and Hall Magnetohydrodynamics, *J. Geophys. Res.*, *102*, 4875, 1997.
- Lottermoser, R.-F., M. Scholer, and A. P. Matthews, Ion kinetic effects in magnetic reconnection: Hybrid simulations, Hall Magnetohydrodynamics, *J. Geophys. Res.*, *103*, 4547, 1998.
- Nakamura, R., et al., Fast flow during current sheet thinning, *Geophys. Res. Lett.*, *29*, 10.1029/2002GL016200, 2002.
- Nakamura, M. S., M. Fujimoto, and K. Maezawa, Ion dynamics and resultant velocity space distributions in the course of magnetotail reconnection, *J. Geophys. Res.*, *103*, 4531, 1998.
- Nagai, T., I. Shinohara, M. Fujimoto, M. Hoshino, Y. Saito, S. Machida, and T. Mukai, Geotail observations of the Hall current system: Evidence of magnetic reconnection in the magnetotail, *J. Geophys. Res.*, *106*, 25,929, 2001.
- Øieroset, M., T. D. Phan, M. Fujimoto, R. P. Lin, and R. P. Lepping, *In situ* detection of collisionless reconnection in the Earth's magnetotail, *Nature*, *412*, 414, 2001.
- Pritchett, P. L., Geospace Environment Modeling magnetic reconnection challenge: Simulations with a full particle electromagnetic code, *J. Geophys. Res.*, *106*, 3783, 2001.
- Rème, H., et al., First multispacecraft ion measurements in and near the Earth's magnetosphere with the identical Cluster ion spectrometry (CIS) experiment, *Ann. Geophys.*, *19*, 1303, 2001.
- Runov, A., R. Nakamura, W. Baumjohann, T. L. Zhang, M. Volwerk, H.-U. Eichelberger, and A. Balogh, Cluster observation of a bifurcated current sheet, *Geophys. Res. Lett.*, submitted, 2002.
- Sato, T., and T. Hayashi, Externally driven magnetic reconnection and a powerful magnetic energy converter, *Phys. Fluids*, *22*, 1189, 1979.
- Semenov, V. S., O. A. Drobysh, and M. F. Heyn, Analysis of time-dependent reconnection in compressible plasmas, *J. Geophys. Res.*, *103*, 11,863, 1998.
- Sergeev, V. A., et al., Current sheet flapping motion and structure observed by Cluster, *Geophys. Res. Lett.*, submitted, 2002.
- Sitnov, M. I., A. S. Sharma, P. N. Guzdar, and P. H. Yoon, Reconnection onset in the tail of Earth's magnetosphere, *J. Geophys. Res.*, *107*, 1256, doi:10.1029/2001JA009148, 2002.
- Sonnerup, B. U. Ö., Magnetic field reconnection, In *Solar System Plasma Physics*, vol. III, edited by L. T. Lanzerotti, C. F. Kennel, and E. N. Parker, pp. 45–108, North-Holland, New York, 1979.
- Terasawa, T., Hall current effect on tearing mode instabilities, *Geophys. Res. Lett.*, *10*, 475, 1983.
- Ugai, M., and T. Tsuda, Magnetic field-line reconnection by localized enhancement of resistivity. Part 1. Evolution in a compressible MHD fluid, *J. Plasma Physics*, *17*, 337, 1977.

W. Baumjohann, R. Nakamura, A. Runov, M. Volwerk, Z. Vörös, and T. L. Zhang, Institut für Weltraumforschung der ÖAW, Schmiedlstr. 6, A-8042, Graz, Austria. (Andrei.Runov@oeaw.ac.at)

B. Klecker and R. A. Treumann, Max-Planck-Institut für extraterrestrische Physik, Garching, Germany.

A. Balogh, Imperial College, London, UK.

K.-H. Glaßmeier, TU Braunschweig, Braunschweig, Germany.

H. Rème, CESR/CNRS, Toulouse, France.

L. Kistler, University of New Hampshire, Durham, NH USA.